HHS Public Access

Author manuscript

Sens Actuators B Chem. Author manuscript; available in PMC 2018 April 01.

Published in final edited form as:

Sens Actuators B Chem. 2017 April ; 242: 658–666. doi:10.1016/j.snb.2016.11.103.

Rapid Measurement of Room Temperature Ionic Liquid Electrochemical Gas Sensor using Transient Double Potential Amperometry

Hao Wan[*], **Heyu Yin**, and **Andrew J. Mason**

Department of Electrical and Computer Engineering, Michigan State University, East Lansing, Michigan, 48824, USA

Abstract

Intense study on gas sensors has been conducted to implement fast gas sensing with high sensitivity, reliability and long lifetime. This paper presents a rapid amperometric method for gas sensing based on a room temperature ionic liquid electrochemical gas sensor. To implement a miniaturized sensor with a fast response time, a three electrode system with gold interdigitated electrodes was fabricated by photolithography on a porous polytetrafluoroethylene substrate that greatly enhances gas diffusion. Furthermore, based on the reversible reaction of oxygen, a new transient double potential amperometry (DPA) was explored for electrochemical analysis to decrease the measurement time and reverse reaction by-products that could cause current drift. Parameters in transient DPA including oxidation potential, oxidation period, reduction period and sample point were investigated to study their influence on the performance of the sensor. Oxygen measurement could be accomplished in 4 s, and the sensor presented a sensitivity of 0.2863 μA/[%O_2] and a linearity of 0.9943 when tested in air samples with different oxygen concentrations. Repeatability and long-term stability were also investigated, and the sensor was shown to exhibit good reliability. In comparison to conventional constant potential amperometry, transient DPA was shown to reduce relative standard deviation by 63.2%. With transient DPA, the sensitivity, linearity, repeatability, measurement time and current drift characteristics demonstrated by the presented gas sensor are promising for acute exposure applications.

Keywords

gas sensor; double potential amperometry; room temperature ionic liquid (RTIL); oxygen detection

1. Introduction

Measurement of ambient gases is of great interests due to the critical role gases play in human health and safety. Individual exposures to gaseous hazards vary significantly in

[*]Corresponding author: wh1816@msu.edu.

different locations and over time, requiring rapid assessment of gas concentrations for vulnerable individuals. For example, toxic gases such as NO_2 and SO_2 may lead to severe cardiac and respiratory symptoms even under low exposure [1, 2], and other gases may directly cause fire and explosion hazards that seriously threaten human safety [3, 4]. Oxygen is an especially important gas that is crucial for human survival, as oxygen deficiency could result in suffocation or death. Furthermore, although oxygen is nontoxic and inflammable, in high concentrations it contributes to fires and explosions acting as an oxidizer. Hence, a reliable gas sensing technology suitable for rapid monitoring of acute exposure is of great interest and necessitates investigation.

Several gas sensing approaches have matured to some level of use in practical industrial applications. Gas chromatography (GC) is a classical and very accurate method for gas separation and quantification. However, GC suffers from large instrument size, high equipment cost, long measurement time, and complicated operation requiring professionally trained personnel [5], making it unsuitable for field applications. Metal oxide semiconductor (MOS) sensors are widely used in commercial gas sensing instruments and exhibit high sensitivity, fast response time, low limit of detection (LOD) and the ability to detect many gas species [6, 7]. Unfortunately, MOS-type gas sensors require heating to increase gas absorption and catalyze gas reaction [8, 9], leading to high power consumption and complicated instrumentation that limits miniaturization and field deployment. The also suffer from long recovery periods that limit real-time operation in practical applications [10]. Optical gas sensors show high sensitivity, good stability and fast response time [11], but they exhibit undesirable size and cost characteristics [10]. In contrast to all of these approaches, electrochemical gas sensors exhibit excellent performance in terms of sensitivity, selectivity and LOD while also being suitable for miniaturization and low cost [12, 13]. However, traditional liquid-electrolyte electrochemical gas sensors suffer from inherent drawbacks in electrolyte evaporation and low gas permeation [14]. Solid electrolytes, such as Nafion membranes [15, 16] and cermet membranes [17] have been investigated as a possible solution to improve gas permeation and electrolyte lifetime, yet they still suffer from limited lifetime [14].

Remarkable benefits can be achieved using room temperature ionic liquid (RTIL) as the electrolyte in electrochemical sensing, since RTILs possess negligible vapor pressure, high thermal stability and a large working potential window [18]. This has encouraged design of many RTIL-based gas sensors that exhibit good performance and demonstrate the value of RTIL. Nevertheless, due RTIL's the high viscosity, low gas permeation still remains a critical issue [12, 14]. Two approaches that have been introduced to address this limitation are decreasing RTIL thickness and avoiding gas permeation through RTIL [19]. In our previous work, the second approach was adopted in a sensor structure with a porous polytetrafluoroethylene (PTFE) substrate through which gas could quickly diffuse [18, 20]. This sensor utilized constant potential amperometry, which is a classic electroanalytical method for gas detection [12, 21] that continuously applies a constant potential while recording the oxidation or reduction current for qualitative and quantitative gas analysis. Although this method can record real-time current changes over a long time period, reaction by-products could accumulate on the surface of the working electrode due to the high viscosity of RTIL [22], which would cause adverse effects on diffusion of target gas and

current response. Furthermore, the measurement by constant potential amperometry is generally conducted after full decay of the charging current that requires long time to stabilize. R. Wang et al. [23] reported a potential-step chronoamperometry method for oxygen detection with reversible reactions, but the 40 s measurement time is still slow for real time health and safety applications. To meet the requirements of acute gas exposure applications, the sensor must respond rapidly to changes in gas concentration and the measurement time must be on the order of seconds. To achieve this goal, this work introduces a new transient double potential amperometry (DPA) method for rapid gas detection with RTIL-based gas sensors by utilizing transient currents and reversible reactions of oxygen.

In this paper, a microfabricated gold interdigitated gas sensor with RTIL electrolyte was used for oxygen detection in air. Porous PTFE was utilized as the sensor substrate to speed target gas diffusion to the sensing electrode, which was formed directly on the porous PTFE using photolithography and custom microfabrication procedures. Cyclic voltammetry and the new transient DPA method were used for sensor characterization and analysis of oxygen measurement performance. A comparison between constant potential amperometry and transient DPA was conducted to validate the superiority of transient DPA in oxygen sensing.

2. Experimental

2.1 Methods and apparatus

High purity nitrogen and compressed air (21% oxygen) were purchased from Airgas Inc. for background gas and oxygen targets, respectively. RTIL 1-butyl-1-methylpyrrolidinium bis-(trifluoromethylsulfonyl)-imide ($[C_4mpy][NTf_2]$) (IOLITEC. Inc.) was chosen as the electrolyte for oxygen sensing because it presented good performance in our previous work [18, 24]. A CHI 760 (CH Instrument, USA) instrument was utilized for all electrochemical tests. A Gas Blender 103 (MCQ Instrument, Italy) was used for automatic gas mixing and flow control. In all tests, the gas flow rate was set to 200 standard cubic centimeter per minute (sccm). Cyclic voltammetry was employed to characterize reactions in RTIL. Transient DPA was implemented for oxygen measurement in air using the multi-potential steps method within the CHI software, as detailed in section 2.3. Constant potential amperometry was employed for comparison with transient DPA.

2.2 Sensor design and implementation

Porous PTFE offers excellent thermal and chemical stability as well as good permeability as a gas sensing substrate [25, 26]. These properties permit the microfabrication of a PTFE-based sensor with fast gas diffusion through PTFE substrate. Microporous PTFE (POREX, USA) with 4 μm pore size and 35% porosity was chosen for the sensor substrate. Gold was chosen as the sensing electrode because it is a readily available material for microfabrication and has shown good performance for oxygen sensing in many other studies [27–29]. To form a complete and miniaturized gas sensor, three electrodes including working electrode (WE), counter electrode (CE) and quasi-reference electrode (RE) were designed to be integrated on the same porous PTFE substrate using the interdigitated structure shown in Fig. 1. Beneath the gold electrode, a thin layer of titanium was included to enhance adhesion

of electrodes to the porous PTFE substrate. Each WE/CE electrode finger was designed to be 1.8 mm × 250 μm, and the gap between electrodes was set to 150 μm. Both WE and CE had three fingers to ensure the intensity of current response in redox reaction. The RTIL electrolyte was designed to be placed on top of the electrode surface while target gases flow directly through porous PTFE substrate. This structure allows the gas to diffuse quickly to the electrode-electrolyte interface, bypassing the need to diffuse through the RTIL layer.

To implement the miniaturized sensor structure, the microfabrication procedures based on our previous work [19] were used to deposit and pattern the electrodes. Due to the porosity and softness of PTFE, the PTFE substrate could not be directly attached to the photoresist (PR) spinner using vacuum. Hence, a temporary glass holder was introduced to support the PTFE substrate. A PR layer of thickness 10 μm was coated on the PTFE surface at a spinning rate 2100 rpm for 60 s (PR AZ4620). A soft bake was then conducted at 95°C for 5 min to enhance photosensitivity of PR. The PR was then patterned by UV exposure for 45 s followed by immersion in AZ300 MIF developer for 4min. Thermal evaporation was used to deposit a 5 nm titanium layer and a 300 nm gold layer on the patterned PR. Finally, the fabricated substrate was immersed in acetone for more than 12 hours and ultrasonic cleaning was performed for 15 min to pattern metals using a full lift-off procedure. After rinsing with acetone, IPA and de-ionized water and drying with N_2, the sensor was ready to be packaged for further test.

The fabricated sensor was mounted on a custom printed circuit board (PCB), as shown in Fig. 3, for convenient electric connection. A hole was drilled through the PCB beneath the electrode area to permit gas flow to the electrodes through the porous sensor substrate. Small drops of epoxy resin were used to adhere the backside of flexible sensor substrate to the PCB at all four corners. Silver conductive epoxy was utilized to route sensor electrode connector pads to wiring on the PCB. After packaging, RTIL was coated on the sensing area of the sensor using a pipette. The sensor was then placed in an oven at 60°C for at least 1 day to remove any gas emission from resins and PCB and to minimize moisture in the RTIL that could interfere with oxygen reactions. The sensor was visually inspected by optical microscopy, and a very rough electrode surface could be observed due to the roughness of PTFE substrate, as shown in Fig. 3b. The width of fabricated fingers was found to range from 270 μm to 280 μm, and the gap between fingers was found to vary from 120 μm to 130 μm. Compared to the designed geometry, the results were slightly wider electrodes and slightly narrower gaps, which is due mainly to the rough surface of porous PTFE that does not allow complete contact between the photomask and the substrate during UV exposure. The scanning electron microscope (SEM) image of the electrode surface is shown in Fig. 3c. Due to the rough surface of PTFE substrate, the titanium/gold electrodes exhibit a very rough surface that is beneficial for enhancing the active sensing area of WE in electrochemical analysis. Moreover, pores observed in the electrodes promote gas diffusion from backside to the three-phase (gas/electrode/electrolyte) interface where reactions take place.

2.3 Transient double potential amperometry

Prior work with RTIL gas sensors has demonstrated two important performance challenges that this study seeks to overcome. The first is long measurement time, generally on the order of 100 s of seconds, using traditional electrochemical methods that must ensure a stable current response after sufficient decay of the charging current and, consequently, impede real-time monitoring applications. The second is reaction byproduct accumulation on the sensor surface leading to drift that ultimately limits the operation lifetime of the sensor. Because by-product generation occurs during sensor measurement, it is exacerbated by long measurement times. Thus, we explored a new means to address both of these challenges by making measurements quickly while reversing by-products to minimize their accumulation. A new transient DPA method was explored to achieve this goal wherein double potentials for both oxygen reduction and superoxide radical ($O_2^{\cdot-}$) oxidation are applied to reverse by-products and transient reaction currents are recorded without waiting for the charging currents to decay. When employed for fast oxygen measurement, transient DPA measurement is based on the reverse reaction of oxygen and superoxide as given by

$$O_2 + e^- \rightleftharpoons O_2^{\cdot-} \quad (1)$$

It is worth noting that the superoxide radical is not stable in a humid atmosphere where reaction with water would suppress the reverse reaction due to its high capacity for reduction as shown by [30]

$$2O_2^{\cdot-} + H_2O \rightarrow O_2 + HO_2^- + OH^- \quad (2)$$

Thus, the reaction of $O_2/O_2^{\cdot-}$ must be verified in RTIL during oxygen measurement in air.

The transient DPA technique that was employed is illustrated in Fig. 4. An oxidation potential E_0 was first applied on WE for the oxidation period T_O to oxidize all reaction products. Subsequently, a reduction potential E_R was applied for the reduction period T_R to reduce oxygen. A typical response current from transient DPA during oxidation and reduction periods is shown in Fig. 4b. Notice the response current experiences fast decay at the beginning of the oxidation and reduction periods due to exponential decay of the charging current. At some relatively long time into each period, the current will stabilize after sufficient decaying of the charging current, as illustrated by the conventional amperometry reduction sample point t_b. In contrast, transient DPA extracts a transient sample current at a much earlier time in the reduction period, represented by t_a, permitting measurements to be made much more quickly, and consequently limiting long-term by-product accumulation.

3. Results and discussions

3.1 Cyclic voltammetry study of oxygen reversibility

In order to characterize the O_2/O_2^- reversibility, cyclic voltammetry was conducted in both N_2 and 100% compressed air backgrounds scanning from −0.4 V to −1.6 V with a scan rate of 0.1 V/s. Cyclic voltammograms of the sensor in both backgrounds are shown in Fig. 5. When tested in N_2, the current response of the sensor is very low and no apparent peak could be observed, denoting a clean gas background with no reactions occurring. In contrast, a distinguishable reduction peak was observed at −0.994 V in 100% air during cathodic scanning, which was assumed to be caused by oxygen reduction. The oxidation anodic scanning peak at −0.638 V was assumed to be caused by oxidation of superoxide radical to oxygen, in accordance with the literature [12]. To establish the potential of the quasi-reference electrode against a standard hydrogen electrode (SHE), the reduction potential of oxygen was used as a reference point. The reduction potential peak of oxygen vs. Ag/AgCl is −0.86 V in ionic liquid [31], and the reduction potential of Ag/AgCl vs. SHE is 0.222 V. Thus, the gold quasi-reference electrode potential against SHE is approximately 0.356 V. Since (2) shows that the superoxide radical will be consumed if water is present, degrading reaction reversibility, this existing oxidation peak also suggests that no moisture exists in the compressed air or the RTIL. The peak-shaped curve during oxidation and reduction indicates a mass transfer controlled process due to the low diffusion coefficient of oxygen and superoxide radical in RTIL. The asymmetry of reduction peak and oxidation peak was attributed to the diffusion difference of oxygen and superoxide in RTIL [31]. These cyclic voltammetry results verify that the reaction between oxygen and superoxide radical is reversible in RTIL by applying different potentials, which establishes the feasibility of reversing superoxide using DPA.

3.2 Parameters study in transient DPA

In transient DPA, parameters including oxidation potential, oxidation period, reduction potential, reduction period and sample point must be defined oxygen detection, as described in section 2.3. First, the reduction potential was set to −1.2 V because the reduction peak of oxygen was observed at −1V in Fig. 5, and this slightly more negative reduction potential will ensure faster reduction reaction.

To define the oxidation potential, different potentials from 0.8 V to 0 V with 0.2 V interval were investigated in 100% compressed air to determine its influence to the sensor performance. The oxidation period and reduction period were preliminarily set to 60 s and 20 s, respectively. Nine repetitive tests were conducted at each oxidation potential, and the averaged current response vs. time is shown in Fig. 6a. When applying a higher oxidation potential, a higher oxidation current amplitude was observed in the oxidation phase, and a higher reduction current amplitude was also observed in the reduction phase. Both oxidation current and reduction current decreased with time within their respective phases due to the decaying of the charging current. To directly compare the influence of different oxidation potentials, currents measured with different oxidation potentials were extracted at three different sample points 1 s, 2 s and 20 s, in the reduction phase. The results plotted in Fig. 6b show that the reduction current response decreases slightly with decreasing oxidation

potential for all the three datasets (at different sample points). The small error bars in nine repetitive tests denote good repeatability with different oxidation potentials, and no significant difference in error was observed at different oxidation potentials. However, oxidation of gold electrodes can occur at high oxidation potentials which could degrade sensor performance. For example, in experiments applying a 0.8 V oxidation potential for two days, the color of the gold electrodes turned black. Subsequent energy-dispersive X-ray spectroscopy showed the surface of the electrodes had a significantly increased amount of oxygen. Moreover, many gaseous components of air that could act as interference sources, e.g. hydrogen, nitric oxide and hydrogen sulfide, have an increased likelihood of oxidizing at higher oxidation potentials. On the other hand, transient DPA study at oxidations potentials below 0.2 V showed low current response. Thus, 0.2 V was chosen as the oxidation potential.

When comparing the current error bars in Fig. 6b for different sample points, notice that errors at 1 s and 2 s, where the currents were recorded in the decay stage, are comparable to the current errors at 20 s, where the currents were recorded at a relatively stable stage. Moreover, the transient current amplitude in the decay stage is much larger than that in the stable stage. These results demonstrate that a transient current in the decaying stage can provide good repeatability and large amplitude for oxygen measurement, while a stable current in conventional constant potential amperometry is not necessarily required. Hence, we chose to reduce the reduction period to 2 s, which greatly shortens the measurement time without sacrificing sensor performance.

Different oxidation periods were also investigated from 60 s to 0.5 s, and the resulting current response vs. time is shown in Fig. 7. In the oxidation phase, the oxidation current decays to a relatively stable stage when the oxidation period is longer than 20 s, while below 20 s the oxidation currents cannot reach a stable point due to an insufficient decaying of the charging current. In the reduction phase, the reduction currents decrease as the oxidation period decreases. The reduction current at sample point $t = 2$ s was extracted to compare the performance at different oxidation periods. As shown in Fig. 7b, currents with oxidation period above 20 s are nearly the same, likely due to achieving full current charging decay in a long oxidation period. In contrast, the reduction current exhibits significant decrease with oxidation periods below 20 s. Moreover, the error in nine repetitive tests increases significantly when shortening the oxidation period below 2 s. An oxidation period of 2 s was selected to minimize both measurement time and repeatability error.

3.3 Quantitative measurement of oxygen with transient DPA

The transient DPA parameters chosen through experimental study were then utilized for quantitative analysis of oxygen in air to validate the feasibility of the method for sensing applications. To ensure consistent working conditions of gas flow equipment, the lowest concentration was set to 0.1% air in a background of N_2. Six different samples were measured with nine repetitive tests, and the averaged current response vs. time is shown in Fig. 8. Currents in both the oxidation phase and the reduction phase were observed to exhibit a gradient response to different concentrations. This occurs because increasing oxygen concentration would lead to more by-products in the reduction phase causing higher

reduction currents, and reversing by-products in the oxidation phase would lead to an according increase in oxidation currents.

The datasets were analyzed using MATLAB to determine the impact of choosing different sample points on the sensitivity, linearity and repeatability of oxygen measurement. As the time of the sample point in the reduction phase was increased from 0.02 s to 2 s, both the current and the sensitivity to oxygen were found to decrease. In contrast, both the linearity and repeatability were found to increase as the sample point time increased. Fig. 8b plots the reduction currents at sample point 1 s and 2 s and shows that the sensitivity of this oxygen sensor, defined as the slope of calibration equation, are 0.3523 μA/[%O_2] and 0.2863 μA/[%O_2] with linearity of 0.9899 and 0.9943, for sample point 1 s and 2 s, respectively. Furthermore, currents at sample point t=2 s present smaller error bars, especially at higher oxygen concentrations, which indicates a better repeatability than the currents at t=1 s. Because charging current is regarded as noise to faradic current in electrochemical analysis, currents at a longer sample point could also provide larger signal to noise ratio and lower LOD. Therefore, a reduction phase sample point of t=2 s was chosen for oxygen measurement, and the sensitivity at this sample point was used for further calculation. It is worth noting that a shorter sample point is also feasible and would obtain higher sensitivity while sacrificing linearity and repeatability.

3.4 Repeatability and stability

Repeatability and long-term stability are important characteristics to evaluate the reliability of a sensor. The short-term repeatability was investigated by performing 20 repetitive tests in 100% air (21% oxygen) with optimized transient DPA and extracting the reduction current at sample point t=2 s. As shown in Fig. 9a, the reduction current is very stable in repetitive tests and the RSD is 0.45%, indicating good repeatability in short-term test. The standard deviation was found to be 0.032 μA, which represents a variation of 0.11% oxygen. To study the long-term stability of the sensor, 4000 sequential tests with optimized transient DPA were conducted in 100% air over 16000 s (4.4 hour) and the reduction current at t=2 s was extracted. Fig. 9b shows that over a long time period the current remains quite stable with an RSD of 2.66% and a standard deviation of 0.167 μA, which represents a variation of only 0.58% oxygen in long-term test. An additional long-term stability test was performed using the same procedure over a 17 day period. The sensor responses in Fig. 9c fluctuate around a mean current with a standard deviation of 0.501 μA (1.75% oxygen), but the results display no significant long-term drift. The variation over time is likely due to changes in the laboratory environmental conditions, especially temperature and humidity, which can have a significant impact on RTIL-based gas sensors [32, 33]. Although laboratory temperature was measured to hold within 2°C, the humidity was found to vary from 38% to 62% over a week. For future laboratory testing, humidity can be accurately controlled using an environmental chamber. For field sensing applications, temperature and humidity compensation [34] can readily be implemented.

3.5 Comparison between constant potential amperometry and transient DPA

The remarkable difference between constant potential amperometry and transient DPA is that an oxidation potential is applied to effectively re-oxidize by-products and decrease by-

product accumulation on the surface of the WE. Since by-products accumulation may interfere with target gas diffusion and cause current drift during measurement, a comparison was made to evaluate the repeatability difference between constant potential amperometry and transient DPA. As shown in Fig. 10a, N_2 was first pumped into the gas chamber for 30 min to eliminate all possible interferants. Afterwards, alternating samples of N_2 and 50% compressed air were introduced for 5 min each in five sequential gas concentration cycles. A constant potential of −1.2 V was applied on the WE, and the current shown in Fig. 10b was recorded with a 10 Hz sampling frequency. In a subsequent test with the same gas concentration cycles, transient DPA was applied at about 4s before each N_2 purge. The recorded transient DPA reduction current vs. time is shown in Fig. 10c, and the inset of Fig. 10c plots the transient DPA reduction current vs. time overlapped for all five gas cycles. Transient DPA exhibits much higher current response mainly because it includes a charging current. From these experimental datasets, values were extracted at the end of each gas cycle for repeatability analysis. For constant potential, response currents of each gas concentration cycle were averaged during the last 2 s of each cycle. For transient DPA, the reduction current at t=2 s was extracted. The repeatability observable in Fig. 10b and the inset of Fig. 10c is compared in Fig. 10d. Over the five gas cycles, the RSD in constant potential amperometry is 4.48% while the RSD in transient DPA is only 1.65%. The deviation of transient DPA is 63.2% less than that of constant potential amperometry, and the apparent downward drift in constant potential is conceivably due to by-products accumulation. In addition to better repeatability, transient DPA benefits from a greatly reduced measurement time compared to constant potential amperometry, which makes it more suitable for real-time monitoring of gaseous hazards.

4. Conclusion

This paper introduced an RTIL-based microfabricated gas sensor and a new transient DPA method for rapid oxygen measurement based on the reverse reaction of oxygen. Parameters in transient DPA have been studied to optimize sensing performance. The sensor and measurement method were tested at different oxygen concentrations and presented good sensitivity, linearity and repeatability. Long-term stability test also validated the good reproducibility of the sensor for oxygen measurement. Compared with constant potential amperometry, this method could largely decrease the measurement time and effectively increase the repeatability by reducing by-product accumulation. Using transient DPA, this miniature electrochemical sensor is suitable for implementation within a wearable microsystem that provides a promising platform for acute gas exposure monitoring in practical applications.

Acknowledgments

The research is supported by National Institutes of Health under NIEHS grant R01ES022302. The authors would like to thank Sam Boling for helpful discussion on MATLAB programming.

References

1. Bernstein JA, Alexis N, Barnes C, Bernstein IL, Bernstein JA, Nel A, Peden D, Diaz-Sanchez D, Tarlo SM, Williams PB. Health effects of air pollution. J Allergy Clin Immunol. 2004; 114:1116–1123. [PubMed: 15536419]
2. Kampa M, Castanas E. Human health effects of air pollution. Environ Pollut. 2008; 151:362–367. [PubMed: 17646040]
3. Han CH, Hong DW, Han SD, Gwak J, Singh KC. Catalytic combustion type hydrogen gas sensor using TiO_2 and UV-LED. Sensors Actuators B Chem. 2007; 125:224–228.
4. Schröder V, Molnarne M. Flammability of gas mixtures: Part 1: Fire potential. J Hazard Mater. 2005; 121:37–44. [PubMed: 15885404]
5. Mcnair, HM., Miller, JM. Basic Gas Chromatography. John Wiley & Sons; New Jersey: 2011.
6. Fine GF, Cavanagh LM, Afonja A, Binions R. Metal oxide semi-conductor gas sensors in environmental monitoring. Sensors. 2010; 10:5469–5502. [PubMed: 22219672]
7. Choi JK, Hwang IS, Kim SJ, Park JS, Park SS, Jeong U, Kang YC, Lee JH. Design of selective gas sensors using electrospun Pd-doped SnO_2 hollow nanofibers. Sensors Actuators, B Chem. 2010; 150:191–199.
8. Wang C, Yin L, Zhang L, Xiang D, Gao R. Metal oxide gas sensors: Sensitivity and influencing factors. Sensors. 2010; 10:2088–2106. [PubMed: 22294916]
9. Batzill M, Diebold U. The surface and materials science of tin oxide. Prog Surf Sci. 2005; 79:47–154.
10. Liu X, Cheng S, Liu H, Hu S, Zhang D, Ning H. A survey on gas sensing technology. Sensors. 2012; 12:9635–9665. [PubMed: 23012563]
11. Werle P, Slemr F, Maurer K, Kormann R, Mücke R, Jänker B. Near- and mid-infrared laser-optical sensors for gas analysis. Opt Lasers Eng. 2002; 37:101–114.
12. Wang Z, Lin P, Baker GA, Stetter J, Zeng X. Ionic liquids as electrolytes for the development of a robust amperometric oxygen sensor. Anal Chem. 2011:7066–7073. [PubMed: 21848335]
13. Hetrick EM, Schoenfisch MH. Analytical chemistry of nitric oxide. Annu Rev Anal Chem. 2009; 2:409–33.
14. Dossi N, Toniolo R, Pizzariello A, Carrilho E, Piccin E, Battiston S, Bontempelli G. An electrochemical gas sensor based on paper supported room temperature ionic liquids. Lab Chip. 2012; 12:153–8. [PubMed: 22076475]
15. Yu C, Wang Y, Hua K, Xing W, Lu T. Electrochemical H_2S sensor with H_2SO_4 pre-treated Nafion membrane as solid polymer electrolyte. Sensors Actuators B Chem. 2002; 86:259–265.
16. Gatty HK, Leijonmarck S, Antelius M, Stemme G, Roxhed N. An amperometric nitric oxide sensor with fast response and ppb-level concentration detection relevant to asthma monitoring. Sensors Actuators, B Chem. 2015; 209:639–644.
17. Kramer KE, Rose-Pehrsson SL, Hammond MH, Tillett D, Streckert HH. Detection and classification of gaseous sulfur compounds by solid electrolyte cyclic voltammetry of cermet sensor array. Anal Chim Acta. 2007; 584:78–88. [PubMed: 17386588]
18. Mu X, Wang Z, Zeng X, Mason AJ. A robust flexible electrochemical gas sensor using room temperature ionic liquid. IEEE Sens J. 2013; 13:3976–3981.
19. Buzzeo MC, Hardacre C, Compton RG. Use of room temperature ionic liquids in gas sensor design. Anal Chem. 2004; 76:4583–4588. [PubMed: 15283606]
20. Li H, Mu X, Wang Z, Guo M, Zeng X, Mason AJ. Room temperature ionic-liquid electrochemical gas sensor array system for real-time mine safety monitoring. IEEE SENSORS Proc. 2013:1–4.
21. Wu FH, Zhao GC, Wei XW. Electrocatalytic oxidation of nitric oxide at multi-walled carbon nanotubes modified electrode. Electrochem Commun. 2002; 4:690–694.
22. Rehman A, Zeng X. Methods and approach of utilizing ionic liquids as gas sensing materials. RSC Adv. 2015; 5:58371–58392.
23. Rong W, Takeyoshi O, Fusao K, Takeo O. A novel amperometric O_2 gas sensor based on supported room- temperature ionic liquid porous polyethylene membrane-coated electrodes. Electroanalysis. 2004; 16:66–72.

24. Mu X, Wang Z, Guo M, Zeng X, Mason AJ. Fabrication of a miniaturized room temperature ionic liquid gas sensor for human health and safety monitoring. IEEE Biomed Circuits Syst Conf. 2012; 1:140–143.
25. Wienecke M, Bunescu M-C, Pietrzak M, Deistung K, Fedtke P. PTFE membrane electrodes with increased sensitivity for gas sensor applications. Synth Met. 2003; 138:165–171.
26. Lu X, Wu S, Wang L, Su Z. Solid-state amperometric hydrogen sensor based on polymer electrolyte membrane fuel cell. Sensors Actuators, B Chem. 2005; 107:812–817.
27. Wadhawan JD, Welford PJ, McPeak HB, Hahn CEW, Compton RG. The simultaneous voltammetric determination and detection of oxygen and carbon dioxide. Sensors Actuators B Chem. 2003; 88:40–52.
28. Hu C, Bai X, Wang Y, Jin W, Zhang X, Hu S. Inkjet printing of nanoporous gold electrode arrays on cellulose membranes for high-sensitive paper-like electrochemical oxygen sensors using ionic liquid electrolytes. Anal Chem. 2012; 84:3745–50. [PubMed: 22424097]
29. Deng Y, Huang W, Chen X, Li Z. Facile fabrication of nanoporous gold film electrodes. Electrochem Commun. 2008; 10:810–813.
30. Switzer EE, Zeller R, Chen Q, Sieradzki K, Buttry DA, Friesen C. Oxygen reduction reaction in ionic liquids: The addition of protic species. J Phys Chem C. 2013; 117:8683–8690.
31. AlNashef IM, Leonard ML, Kittle MC, Matthews Ma, Weidner JW. Electrochemical generation of superoxide in room-temperature ionic liquids. Electrochem Solid-State Lett. 2001; 4:D16.
32. Rogers EI, Huang X, Dickinson EJF, Hardacre C, Compton RG. Investigating the mechanism and electrode kinetics of the oxygen|superoxide ($O_2|O_2^{\cdot-}$) couple in various room-temperature ionic liquids at gold and platinum electrodes in the temperature range 298–318 K. J Phys Chem C. 2009; 113:17811–17823.
33. Zevenbergen MAG, Wouters D, Dam VAT, Brongersma SH, Crego-Calama M. Electrochemical sensing of ethylene employing a thin ionic-liquid layer. Anal Chem. 2011; 83:6300–6307. [PubMed: 21721532]
34. Sohn JH, Atzeni M, Zeller L, Pioggia G. Characterisation of humidity dependence of a metal oxide semiconductor sensor array using partial least squares. Sensors Actuators, B Chem. 2008; 131:230–235.

Biographies

Hao Wan received the B.S. and Ph.D. degree in Biomedical Engineering from Huazhong University of Science and Technology, Wuhan, China and Zhejiang University, Hangzhou, China in 2010 and 2015, respectively. He is currently a postdoc in the Department of Electrical and Computer Engineering, Michigan State University, East Lansing, MI, USA. His research interests are sensor microfabrication, electrochemical sensing and instrument development in environmental monitoring applications.

Heyu Yin revived the B.S. degree in Engineering management from Hubei University, Wuhan, China and Master degree in Microelectronics and Nanoelectronics from Tsinghua University, Beijing, China. He is currently a Ph.D. student in the Department of Electrical and Computer Engineering, Michigan State University, East Lansing, MI, USA. His research interests are electrochemical sensor and lab-on-CMOS integration for portable biosensing and environmental monitoring application.

Andrew J. Mason received the B.S. degree in physics with highest distinction from Western Kentucky University, Bowling Green, KY, USA, in 1991, the BSEE (honors) from the Georgia Institute of Technology, Atlanta, GA, USA, in 1992, and the M.S. and Ph.D. degrees in electrical engineering from the University of Michigan, Ann Arbor, MI, USA, in

1994 and 2000, respectively. Hi is currently a full professor in the Department of Electrical and Computer Engineering, Michigan State University, East Lansing, MI, USA. His research explores mixed-signal circuits, microfabricated structures, and machine learning algorithms for integrated microsystems in biomedical, environmental monitoring, and sustainable lifestyle applications.

Highlights

- An electrochemical gas sensor was fabricated with porous polytetrafluoroethylene as the substrate and room temperature ionic liquid as the electrolyte.
- A new transient double potential amperometry was explored to decrease measurement time and reverse reaction by-products.
- The sensor was validated to present good sensitivity, high linearity and good repeatability with the new method.

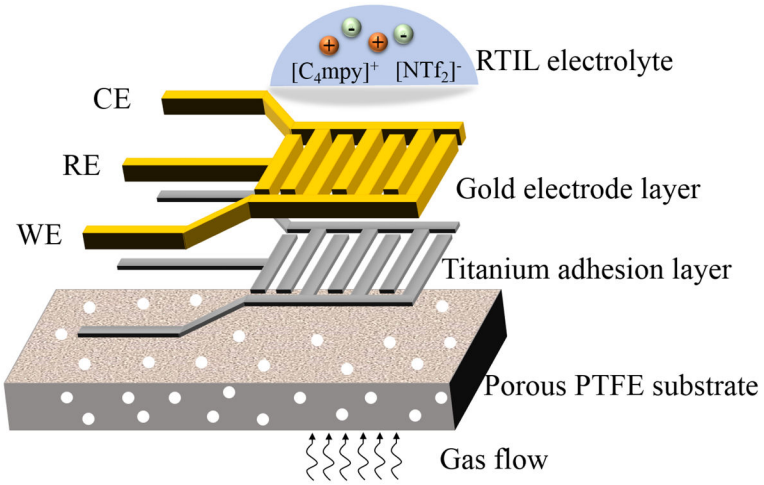

Figure 1.
Structural schematic of the microfabricated RTIL gas sensor.

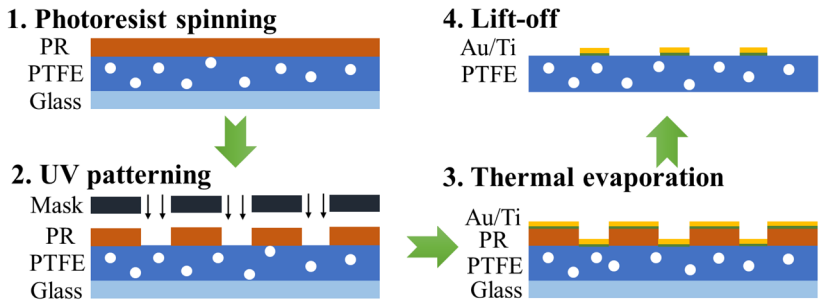

Figure 2.
Microfabrication process flow for formation of sensor electrodes on porous PTFE substrate.

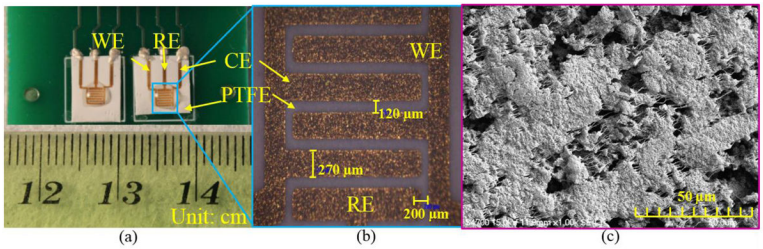

Figure 3.

Fabricated RTIL-based electrochemical gas sensor: (a) gas sensors packaged on a PCB; (b) optical microscope view of gold interdigitated electrodes; and (c) SEM image of the rough electrode surface.

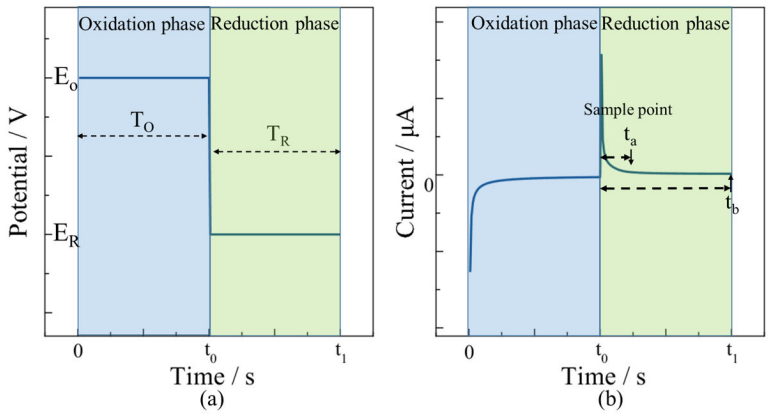

Figure 4.

Principle and parameters of transient DPA for reversible reactions: (a) The potential vs. time applied on WE; (b) typical WE current response vs. time. E_O, oxidation potential; E_R, reduction potential; T_O, oxidation period; T_R, reduction period; t_a and t_b, sample points in the reduction phase.

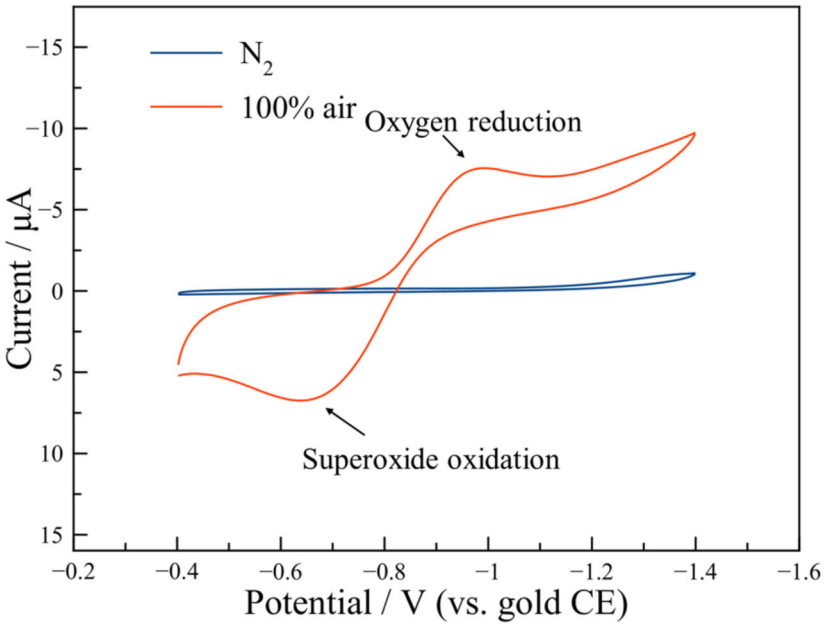

Figure 5.
Cyclic voltammetry test of microfabricated RTIL gas sensor in N_2 and 100% compressed air.

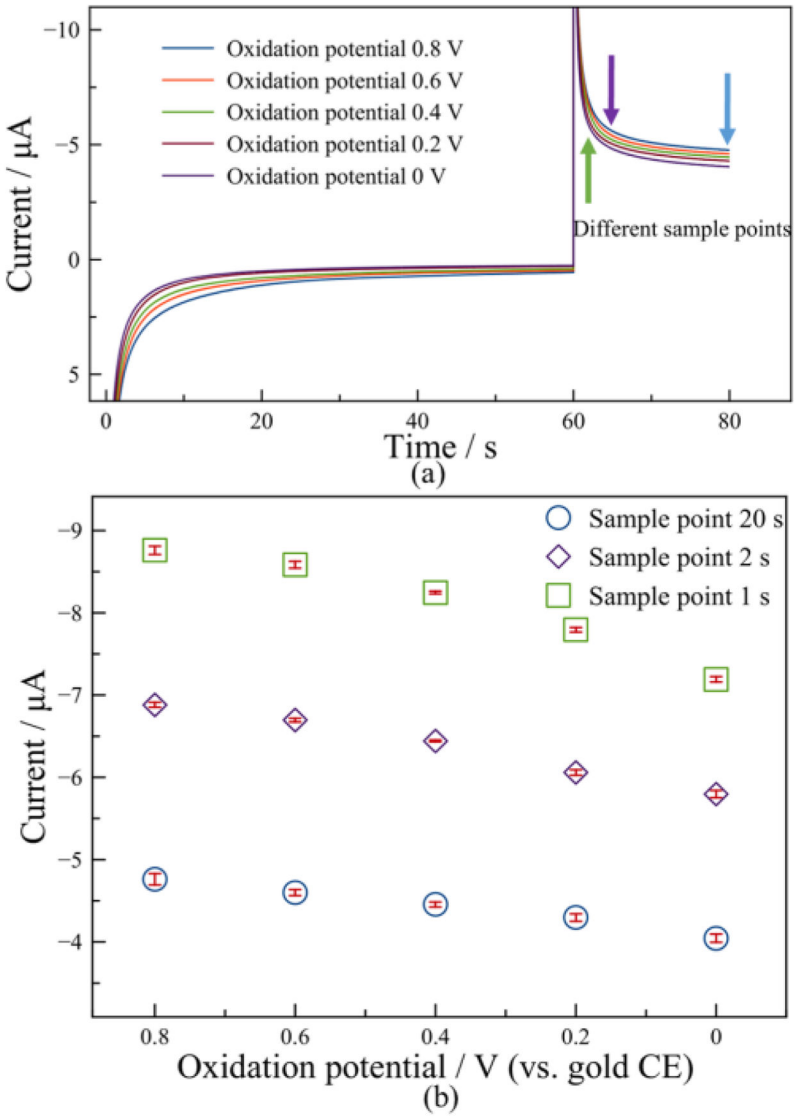

Figure 6.

Study of effect of oxidation potential: (a) Plot of current response vs. time at different oxidation potentials; (b) Plot of reduction current vs. oxidation potential at sample points *t*=1 s, 2 s and 20 s.

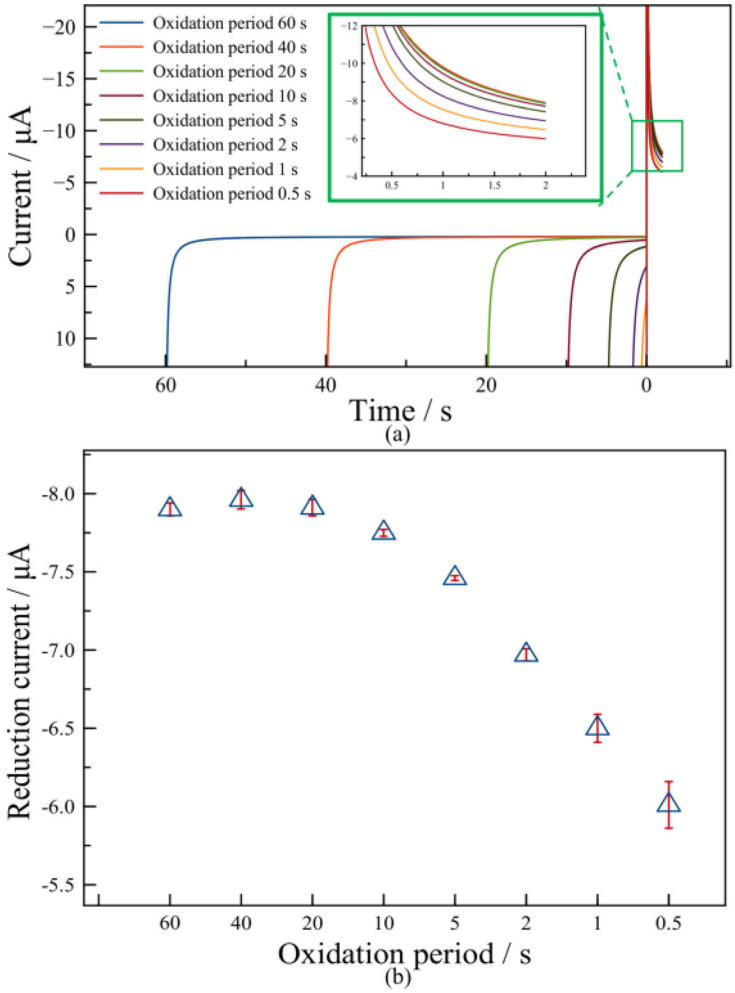

Figure 7.

Study of effect of oxidation period: (a) Plot of current response vs. time for different oxidation periods. The inset magnifies the reduction phase current; (b) Plot of reduction current vs. oxidation period at sample point t=2 s

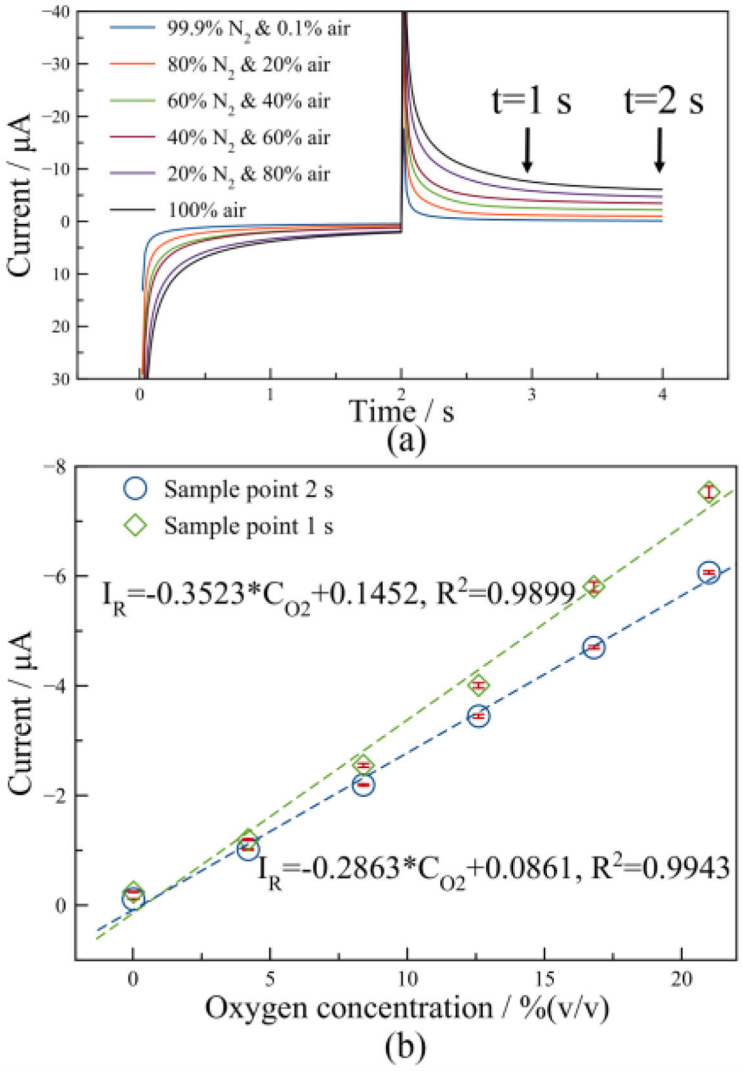

Figure 8.

(a) Current response of the microfabricated RTIL gas sensor for different air (oxygen) concentrations; (b) The oxygen calibration curve at sample points *t*=1 s and 2 s.

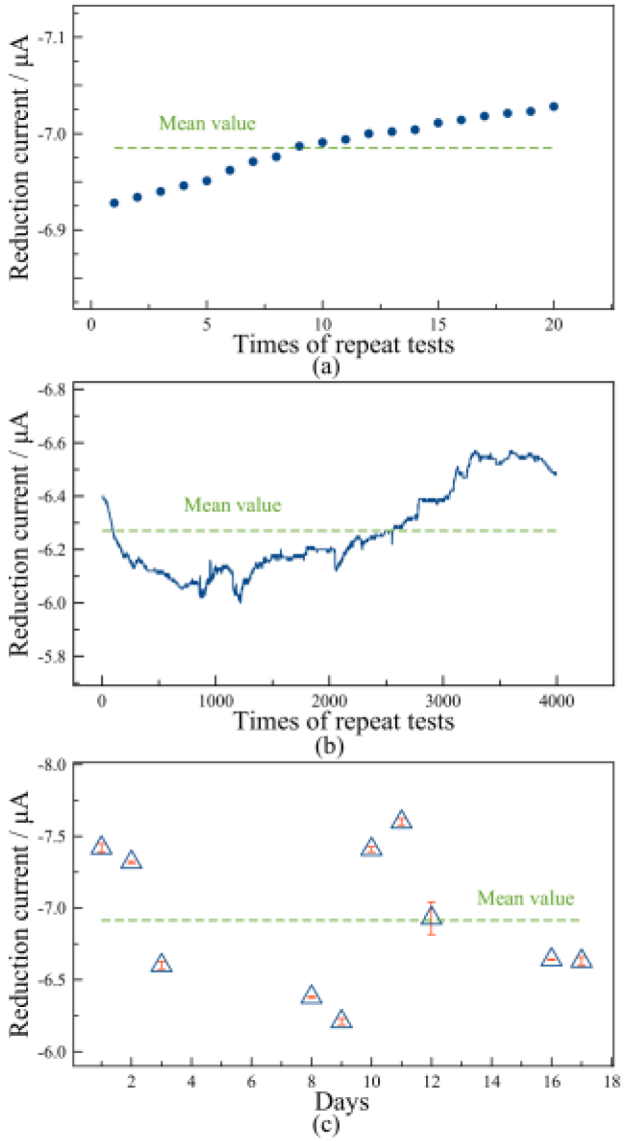

Figure 9.

Study of short-term repeatability and long-term stability using transient DPA in 100% air (21% oxygen) with reduction current extracted at t=2 s: (a) 20 repetitive tests; (b) 4000 repetitive tests; (c) Multiple tests over 17 days.

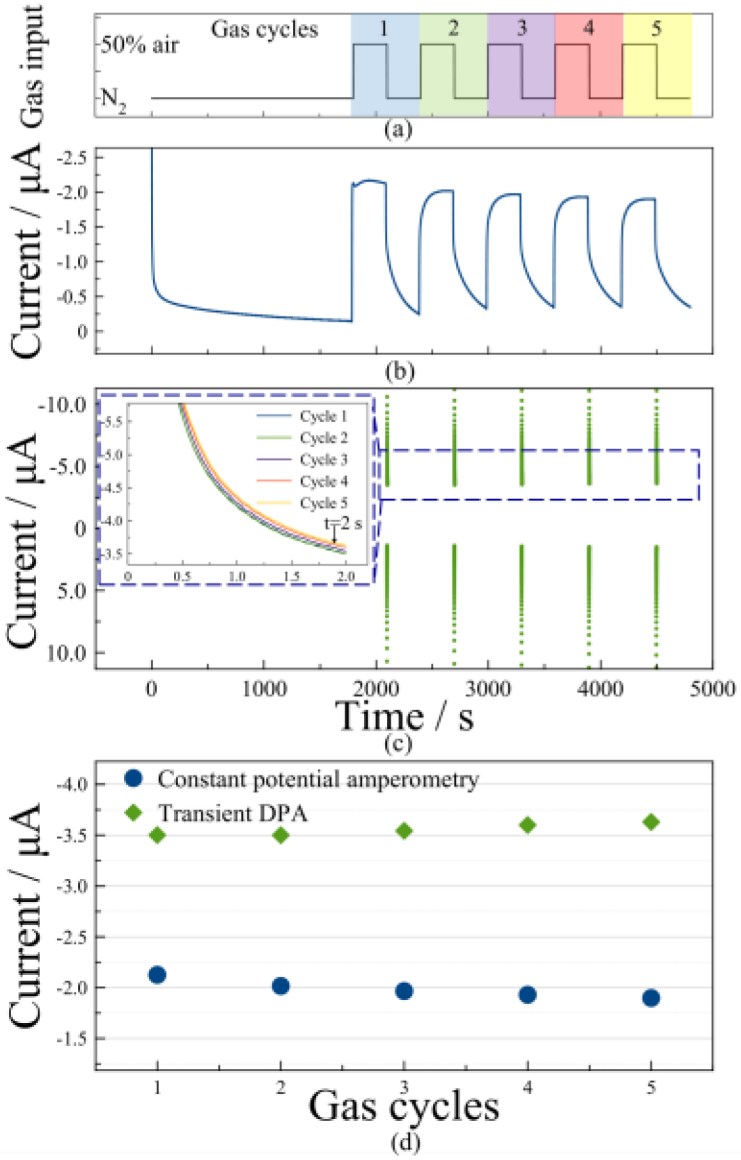

Figure 10.

Performance comparison of constant potential amperometry and transient DPA for five cycles of alternating gas concentrations between N_2 and 50% air: (a) gas concentration cycles vs. time; (b) constant potential amperometry current response vs. time; (c) transient DPA current response vs. time; (d) reduction current comparison using constant potential amperometry (blue) and transient DPA (green). The inset in (c) shows the transient DPA reduction current plots overlapped for five gas cycles.